

Verification of Braginskii Closures in NIMROD on MHD Waves

K. J. Bunkers and C. R. Sovinec

University of Wisconsin-Madison
Center for Plasma Theory and Computation
Report UW-CPTC 17-8

November 21, 2017

NOTICE

This report was prepared as an account of work sponsored by an agency of the United States Government. Neither the United States Government, nor any of their employees, makes any warranty, express or implied, or assumes any legal liability for the accuracy, completeness, or usefulness of any information, apparatus, product, or process disclosed, or represents that its use would not infringe privately owned rights. Reference herein to any specific commercial product, process, or service by trade name, trademark, manufacturer, or otherwise does not necessarily constitute or imply its endorsement, recommendation, or favoring by the United States Government or any agency thereof. The views and opinions of authors expressed herein do not necessarily state or reflect those of the United States Government or any agency thereof.

1 Summary of Methods and Results

In order to test the implementation of the viscosity in NIMROD, the dispersion relations for viscous and thermally diffusive MHD are used to predict linear growth rates and frequencies of waves in a simple homogeneous system. We begin with viscous MHD, ignoring thermal diffusive and resistive effects. This system can be written as (single fluid MHD)

$$\frac{\partial n}{\partial t} + \nabla \cdot (n\mathbf{V}) = 0 \quad (1)$$

$$mn \frac{\partial \mathbf{V}}{\partial t} + mn \mathbf{V} \cdot \nabla \mathbf{V} = \mathbf{J} \times \mathbf{B} - \nabla \cdot \overset{\leftrightarrow}{\mathbf{P}} \quad (2)$$

$$n \frac{dT}{dt} = -(\gamma - 1)nT \nabla \cdot \mathbf{V} - (\gamma - 1) \nabla \cdot \mathbf{q} \quad (3)$$

$$\mu_0 \mathbf{J} = \nabla \times \mathbf{B} \quad (4)$$

$$\mathbf{E} = -\mathbf{V} \times \mathbf{B} \quad (5)$$

$$\frac{\partial \mathbf{B}}{\partial t} = -\nabla \times \mathbf{E} \quad (6)$$

$$\nabla \cdot \mathbf{B} = 0 \quad (7)$$

where γ is the adiabatic index, set to 5/3 in usual MHD circumstances. Our closure in this case becomes

$$\overset{\leftrightarrow}{\mathbf{P}} = \mathbb{1}p + \overset{\leftrightarrow}{\mathbf{\Pi}} \quad (8)$$

$$p = nT \quad (9)$$

$$\nabla \cdot \mathbf{q} = 0 \quad (10)$$

$$(11)$$

The stress tensor $\overset{\leftrightarrow}{\mathbf{\Pi}}$ is divided into different components in the NIMROD implementation. In this paper, they are designated as

$$\overset{\leftrightarrow}{\mathbf{\Pi}}_{\text{kin}} = -\eta_{\text{kin}} \nabla \nabla \quad (12)$$

$$\overset{\leftrightarrow}{\mathbf{\Pi}}_{\text{iso}} = -\eta_{\text{iso}} \overset{\leftrightarrow}{\mathbf{W}} \quad (13)$$

$$\overset{\leftrightarrow}{\mathbf{\Pi}}_{\parallel} = -\frac{3}{2}\eta_0 (\overset{\leftrightarrow}{\mathbf{W}} : \hat{\mathbf{b}}\hat{\mathbf{b}}) (\hat{\mathbf{b}}\hat{\mathbf{b}} - \mathbb{1}/3) \quad (14)$$

$$\overset{\leftrightarrow}{\mathbf{\Pi}}_{\text{gyro}} = \frac{1}{2}\eta_3 \left((\hat{\mathbf{b}} \times \overset{\leftrightarrow}{\mathbf{W}}) \cdot (\kappa_{\wedge} \hat{\mathbf{b}}\hat{\mathbf{b}} + \mathbb{1}) - (\kappa_{\wedge} \hat{\mathbf{b}}\hat{\mathbf{b}} + \mathbb{1}) \cdot (\overset{\leftrightarrow}{\mathbf{W}} \times \hat{\mathbf{b}}) \right) \quad (15)$$

$$\overset{\leftrightarrow}{\mathbf{\Pi}}_{\perp} = -\eta_1 \left((\mathbb{1} + \kappa_{\perp} \hat{\mathbf{b}}\hat{\mathbf{b}}) \cdot \overset{\leftrightarrow}{\mathbf{W}} \cdot (\mathbb{1} + \kappa_{\perp} \hat{\mathbf{b}}\hat{\mathbf{b}}) + \frac{1}{2}(\mathbb{1} + \kappa_{\vee} \hat{\mathbf{b}}\hat{\mathbf{b}}) \hat{\mathbf{b}}\hat{\mathbf{b}} : \overset{\leftrightarrow}{\mathbf{W}} \right) \quad (16)$$

$$\overset{\leftrightarrow}{\mathbf{\Pi}}_{\parallel}^b = -\frac{1}{2} \overset{\leftrightarrow}{\mathbf{W}} : \hat{\mathbf{b}}\hat{\mathbf{b}} (\alpha_1 \hat{\mathbf{b}}\hat{\mathbf{b}} - \alpha_2 \mathbb{1}/3) \quad (17)$$

$$\overset{\leftrightarrow}{\mathbf{\Pi}}_{\perp}^b = -\eta_1 \left(\overset{\leftrightarrow}{\mathbf{W}} + \kappa_{\perp}^b \left(\hat{\mathbf{b}}\hat{\mathbf{b}} \cdot \overset{\leftrightarrow}{\mathbf{W}} + \overset{\leftrightarrow}{\mathbf{W}} \cdot \hat{\mathbf{b}}\hat{\mathbf{b}} \right) \right) \quad (18)$$

Here $\overset{\leftrightarrow}{\mathbf{W}} = \nabla \mathbf{V} (\nabla \mathbf{V})^{\top} - \frac{2}{3} \nabla \cdot \mathbf{V}$ is the rate-of-strain tensor. Note that when the superscript b is on a component, it indicates this is how NIMROD actually handles that portion of the NIMROD $\overset{\leftrightarrow}{\mathbf{\Pi}}$

tensor. This means

$$\overset{\leftrightarrow}{\Pi}^{\text{NIMROD}} = \overset{\leftrightarrow}{\Pi}_{\parallel}^b + \overset{\leftrightarrow}{\Pi}_{\perp}^b + \overset{\leftrightarrow}{\Pi}_{\wedge}^b \quad (19)$$

$$\overset{\leftrightarrow}{\Pi} = \overset{\leftrightarrow}{\Pi}_{\parallel} + \overset{\leftrightarrow}{\Pi}_{\perp} + \overset{\leftrightarrow}{\Pi}_{\wedge} \quad (20)$$

$$\overset{\leftrightarrow}{\Pi} = \overset{\leftrightarrow}{\Pi}^{\text{NIMROD}} \quad (21)$$

(note that if $\eta_{\text{kin,iso}} \neq 0$ we simply add that into $\overset{\leftrightarrow}{\Pi}$, as necessary as they are identical in analytic and NIMROD implementations). From now on, let us refer to the superscript b equations, as they are the relevant calculations for testing dispersion relations.

The various coefficients are

$$\kappa_{\perp} = \kappa_{\perp}^b = \frac{\eta_2}{\eta_1} - 1 \equiv \gamma_{\perp} - 1 \quad (22)$$

$$\kappa_{\vee} = -2 \left(\frac{\eta_2}{\eta_1} \right)^2 - 1 \equiv -2\gamma_{\perp}^2 - 1 \quad (23)$$

$$\kappa_{\wedge} = 2 \frac{\eta_4}{\eta_3} - 1 \equiv 2\gamma_{\wedge} - 1 \quad (24)$$

$$\alpha_1 = 3\eta_0 + \eta_1 - 4\eta_2 = 3\eta_0 - (4\eta_2 - \eta_1) = 3\eta_0 - (4\gamma_{\perp} - 1)\eta_1 \quad (25)$$

$$\alpha_2 = \eta_0 - \eta_1 \quad (26)$$

$$x_i = \Omega_i \tau_i = \frac{q_i B}{m_i} \tau_i \quad (27)$$

Here x_i is the ion magnetization. The coefficients η_j ($j = 0, 1, 2, 3, 4$) all differ depending on the closure and whether NIMROD is running linearly or nonlinearly.

For these calculations we will use η_j that are not varying in time or space. Let \mathbf{B}_0 be constant in space and time with $\hat{\mathbf{b}} = \mathbf{B}_0/B_0$. We then linearize with $q = q_0 + q_1 e^{-i\omega t + i\mathbf{k} \cdot \mathbf{x}}$ for $q_1/q_0 \ll 1$ for any quantity q except for \mathbf{V} where $\mathbf{V}_0 = \mathbf{0}$ (no background flow). We can further define the sound speed (v_S) and Alfvén speed (v_A) as

$$v_S^2 = \frac{T_0 \gamma}{m \mu_0} \quad (28)$$

$$v_A^2 = \frac{B_0^2}{m n_0 \mu_0} \quad (29)$$

This system and linearization yields

$$\frac{n_1}{n_0} = \frac{\mathbf{k} \cdot \mathbf{V}_1}{\omega}, \quad \frac{T_1}{T_0} = \frac{(\gamma - 1)(\mathbf{k} \cdot \mathbf{V}_1)}{\omega}, \quad \frac{P_1}{P_0} = \frac{\gamma(\mathbf{k} \cdot \mathbf{V}_1)}{\omega} \quad (30)$$

$$\mathbf{B}_1 = \frac{-\mathbf{V}_1(\mathbf{k} \cdot \mathbf{B}_0) + \mathbf{B}_0(\mathbf{k} \cdot \mathbf{V}_1)}{\omega} \quad (31)$$

$$\begin{aligned} -i\omega m n_0 \mathbf{V}_1 = & -i\mathbf{k}(\mathbf{B}_1 \cdot \mathbf{B}_0 + n_0 T_1 + n_1 T_0) + i\mathbf{B}_1(\mathbf{k} \cdot \mathbf{B}_0) - (\nabla \cdot \overset{\leftrightarrow}{\Pi})_{\text{lin}} \\ (\omega^2 - k_{\parallel}^2 v_A^2) \mathbf{V}_1 + i \frac{\omega}{m n_0} (\nabla \cdot \overset{\leftrightarrow}{\Pi})_{\text{lin}} = & \mathbf{k} \left[v_A^2 (\mathbf{k} \cdot \mathbf{V}_1) - v_A^2 (\mathbf{k} \cdot \hat{\mathbf{b}}) (\mathbf{V}_1 \cdot \hat{\mathbf{b}}) + v_S^2 (\mathbf{k} \cdot \mathbf{V}_1) \right] \\ & - v_A^2 (\mathbf{k} \cdot \mathbf{V}_1) (\mathbf{k} \cdot \hat{\mathbf{b}}) \hat{\mathbf{b}} \end{aligned} \quad (32)$$

$$\begin{aligned}
 (\nabla \cdot \overset{\leftrightarrow}{\Pi})_{\text{lin}} = & k^2(\eta_{\text{kin}} + \eta_{\text{iso}})\mathbf{V}_1 + \frac{\eta_{\text{iso}} + \eta_{\parallel}}{3}(\mathbf{k} \cdot \mathbf{V}_1)\mathbf{k} + \frac{\eta_{\text{gyro}}}{2} \left[(\mathbf{k} \cdot \hat{\mathbf{b}} \times \mathbf{V}_1)\mathbf{k} + (\mathbf{k} \cdot \mathbf{V}_1)(\hat{\mathbf{b}} \times \mathbf{k}) \right. \\
 & \left. + k^2\hat{\mathbf{b}} \times \mathbf{V}_1 \right] + \eta_{\perp} \left\{ [k^2 + \kappa_{\perp}(\mathbf{k} \cdot \hat{\mathbf{b}})^2]\mathbf{V}_1 + [(\kappa_{\perp} + 1)(\mathbf{k} \cdot \hat{\mathbf{b}})(\mathbf{V}_1 \cdot \hat{\mathbf{b}})]\mathbf{k} + \left[\kappa_{\perp}k^2(\mathbf{V}_1 \cdot \hat{\mathbf{b}}) \right. \right. \\
 & \left. \left. - \frac{\kappa_{\perp} + 2\kappa_{\perp}^2 + \kappa_{\vee}}{3}(\mathbf{k} \cdot \hat{\mathbf{b}})(\mathbf{k} \cdot \mathbf{V}_1) + (2\kappa_{\perp}^2 + \kappa_{\vee})(\mathbf{k} \cdot \hat{\mathbf{b}})^2(\mathbf{V}_1 \cdot \hat{\mathbf{b}}) \right] \hat{\mathbf{b}} \right\}
 \end{aligned} \tag{33}$$

For standing waves, we use that for a traveling wave with dependence on ω given by $f(\omega)$, that $f_{\text{standing wave}} \equiv f_{\text{st}} = \frac{1}{2}[f(\omega) + f(\omega = -\omega^*)]$ where $\omega = \omega_R + i\omega_I$.

For convenience let $\hat{\eta} = \eta/(mn_0)$.

We then find the dispersion relation for sound waves ($\mathbf{k} = k_{\parallel}\hat{\mathbf{b}}$, $\mathbf{V} = v_{\parallel}\hat{\mathbf{b}}$) yielding

$$\omega^2 + i\omega k_{\parallel}^2 \left(\hat{\eta}_{\text{kin}} + \frac{4}{3}\hat{\eta}_{\text{iso}} + \frac{4}{3}\hat{\eta}_{\parallel} + \epsilon\hat{\eta}_{\perp} \frac{4 + 8\kappa_{\perp}}{3} \right) - k_{\parallel}^2 v_S^2 = 0 \tag{34}$$

In this relation, $\epsilon = 1$ if $\eta_{\perp} \neq 0$ and $\eta_{\parallel} = 0$; otherwise $\epsilon = 0$. That is ϵ is nonzero only for calculations isolating the perpendicular component of the stress tensor.

The dispersion relation for shear Alfvén waves ($\mathbf{k} = k_{\parallel}\hat{\mathbf{b}}$, $\mathbf{V} \cdot \hat{\mathbf{b}} = 0$ [note that $\mathbf{V} \cdot \hat{\mathbf{b}} = 0$ and $\mathbf{V} \cdot \mathbf{k} = 0$ are what is necessary for a shear Alfvén wave]) yields

$$(\omega^2 - k_{\parallel}^2 v_A^2 + i\omega k_{\parallel}^2 \hat{\eta}_{\text{eff}} - \alpha_{\wedge} \omega k_{\parallel}^2 \hat{\eta}_{\text{gyro}})(\omega^2 - k_{\parallel}^2 v_A^2 + i\omega k_{\parallel}^2 \hat{\eta}_{\text{eff}} + \alpha_{\wedge} \omega k_{\parallel}^2 \hat{\eta}_{\text{gyro}}) = 0 \tag{35}$$

$$\hat{\eta}_{\text{eff}} = \hat{\eta}_{\text{kin}} + \hat{\eta}_{\text{iso}} + \hat{\eta}_{\perp}(1 + \kappa_{\perp}) \tag{36}$$

The dispersion relation for compressional Alfvén waves is ($\mathbf{k} \cdot \hat{\mathbf{b}} = 0$, $\mathbf{V} \cdot \hat{\mathbf{b}} = 0$, letting $\hat{\mathbf{b}} = \hat{\mathbf{z}}$)

$$\begin{aligned}
 \omega^4 + i\omega^3 F^2 - \omega^2(v_W^2 k^2 + F_x F_y + \hat{\eta}_{\text{gyro}}^2 k^4 - \delta^2 k_x^2 k_y^2) \\
 - i\omega v_W^2 (F_x k_y^2 + F_y k_x^2 - 2\delta k_x^2 k_y^2) = 0
 \end{aligned} \tag{37}$$

where

$$F_i = k^2(\hat{\eta}_{\text{kin}} + \hat{\eta}_{\text{iso}} + \hat{\eta}_{\perp}) + \frac{\hat{\eta}_{\text{iso}} + \hat{\eta}_{\parallel} + \hat{\eta}_{\perp}}{3} k_i^2 \tag{38}$$

$$F^2 = 2k^2(\hat{\eta}_{\text{kin}} + \hat{\eta}_{\text{iso}} + \hat{\eta}_{\perp}) + k^2 \frac{\hat{\eta}_{\text{iso}} + \hat{\eta}_{\parallel} + \hat{\eta}_{\perp}}{3} \tag{39}$$

$$\delta = \frac{\hat{\eta}_{\text{iso}} + \hat{\eta}_{\parallel} + \hat{\eta}_{\perp}}{3} \tag{40}$$

$$v_W^2 = v_A^2 + v_S^2 \tag{41}$$

Also note that the numerical parameters for all calculations was using a doubly periodic box (`gridshape='rect'`, `geom='lin'`, and `periodicity='both'`) with $x \in [0, 1]$, $y \in [0, 2\pi]$, `mx = my = 8`, `nxbl = 2`, `nybl = 1`, and a single Fourier mode. The timestep was usually `dtm = dt_initial = 10-2` or smaller.

2 NIMROD Calculations Run Linearly

For calculations run linearly with NIMROD, we have (`visc_model = fixed` was used, but for completeness, the temperature dependent (`tdep`) forms are also presented)

$$\eta_0 \stackrel{\text{fixed}}{=} \eta_{\parallel} \stackrel{\text{tdep}}{=} \eta_{\parallel} \left(\frac{T_i}{T_{\text{ref}}} \right)^{5/2} \quad (42)$$

$$\eta_1 \stackrel{\text{fixed}}{=} \eta_{\perp} \stackrel{\text{tdep}}{=} \frac{\eta_{\perp}}{B^2} \sqrt{\frac{T_{\text{ref}}}{T_i}} \quad (43)$$

$$\eta_2 = 4\eta_1 \quad (44)$$

$$\eta_3 = \frac{\eta_{\text{gyro}} n_i T_i}{2\Omega_i} \quad (45)$$

$$\eta_4 = 2\eta_3 \quad (46)$$

Here `par_visc` = η_{\parallel} , `prp_visc` = η_{\perp} , `gyr_visc` = η_{gyro} , `k_pll_ref_t` = T_{ref} have been used.

For calculational convenience, a normalized system was used where

$$m_i = c = \mu_0 = k_B = q = 1 \quad (47)$$

$$m_e = 0 \quad (48)$$

which corresponds to

$$\text{mi_input} = \text{kblz_input} = \text{mu0_input} = \text{chrg_input} = \text{c_input} = 1 \quad (49)$$

$$\text{me_input} = 0 \quad (50)$$

Then

$$\beta = \text{beta} = 15 \quad (51)$$

$$B_0 = \text{be0} = 1 \quad (52)$$

$$n_0 = \text{ndens} = 1 \quad (53)$$

is chosen, leaving the default adiabatic index of $\gamma = 5/3$. This leads to (with `pe_frac` = 0.5)

$$v_A^2 = \frac{B_0^2}{(m_i + m_e)\mu_0 n_0} = \frac{1^2}{(1+0)(1)(1)} = 1 \quad (54)$$

$$p_0 = \frac{\beta}{2\mu_0} = \frac{15}{2(1)} = 7.5 \quad (55)$$

$$T_0 = \frac{p_0}{n_0} = \frac{7.5}{1} = 7.5 \quad (56)$$

$$T_i = (1 - \text{pe_frac})T_0 = \frac{15}{4} = 3.75 = T_e \quad (57)$$

$$v_S^2 = \frac{\gamma T_0}{m_{\text{tot}}} = B_0^2 \frac{\gamma \beta}{2\mu_0 n_0 (m_i + m_e)} = 1^2 \frac{\frac{5}{3} 15}{2(1)(1)(1+0)} = \frac{25}{2} = 12.5 \quad (58)$$

For all waves, we assume $\mathbf{k} = k\hat{\mathbf{y}}$. Remember that

$$\mathbf{B}_R = \mathbf{bex} = B_0 \sin(\pi\theta_b) \cos(\pi\phi_b) \quad (59)$$

$$\mathbf{B}_Z = \mathbf{bey} = B_0 \sin(\pi\theta_b) \sin(\pi\phi_b) \quad (60)$$

$$\mathbf{B}_\varphi = \mathbf{bez} = B_0 \cos(\pi\theta_b) \quad (61)$$

For sound waves ($\mathbf{k} = k_{\parallel}\hat{\mathbf{b}}$, $\mathbf{V}_1 = v_{\parallel}\hat{\mathbf{b}}$), we have

$$\theta_b = \text{thetab} = 0.5 \quad (62)$$

$$\phi_b = \text{phib} = 0.5 \quad (63)$$

So that we have $\mathbf{B}_0 = B_0\hat{\mathbf{y}}$ for the sound waves.

For shear Alfvén waves ($\mathbf{k} = k_{\parallel}\hat{\mathbf{b}}$, $\mathbf{V}_1 \cdot \hat{\mathbf{b}} = 0$), we have

$$\theta_b = \text{thetab} = 0.5 \quad (64)$$

$$\phi_b = \text{phib} = 0.5 \quad (65)$$

So that we have $\mathbf{B}_0 = B_0\hat{\mathbf{y}}$ for the shear waves.

For compressional Alfvén waves ($\mathbf{k} \cdot \hat{\mathbf{b}} = 0$ and $\mathbf{V}_1 \cdot \hat{\mathbf{b}} = 0$).

$$\theta_b = \text{thetab} = 0.5 \quad (66)$$

$$\phi_b = \text{phib} = 0.0 \quad (67)$$

So that we have $\mathbf{B}_0 = B_0\hat{\mathbf{x}}$ for the compressional waves. This will mean the contributing perturbations for velocity are purely in $\hat{\mathbf{y}}$.

Also note that all of these are $k = 1$ modes.

Then we test each component of $\overset{\leftrightarrow}{\Pi}^{\text{NIMROD}}$ separately for each wave for various values.

In all following figures the frequency $f_R = \omega_R/(2\pi)$ and the damping rate $\gamma = -\omega_I$ (so growth rates would be negative) are shown. ‘‘Actual’’ comes from the analytic dispersion relations, while ‘‘measured’’ is what is observed from NIMROD output.

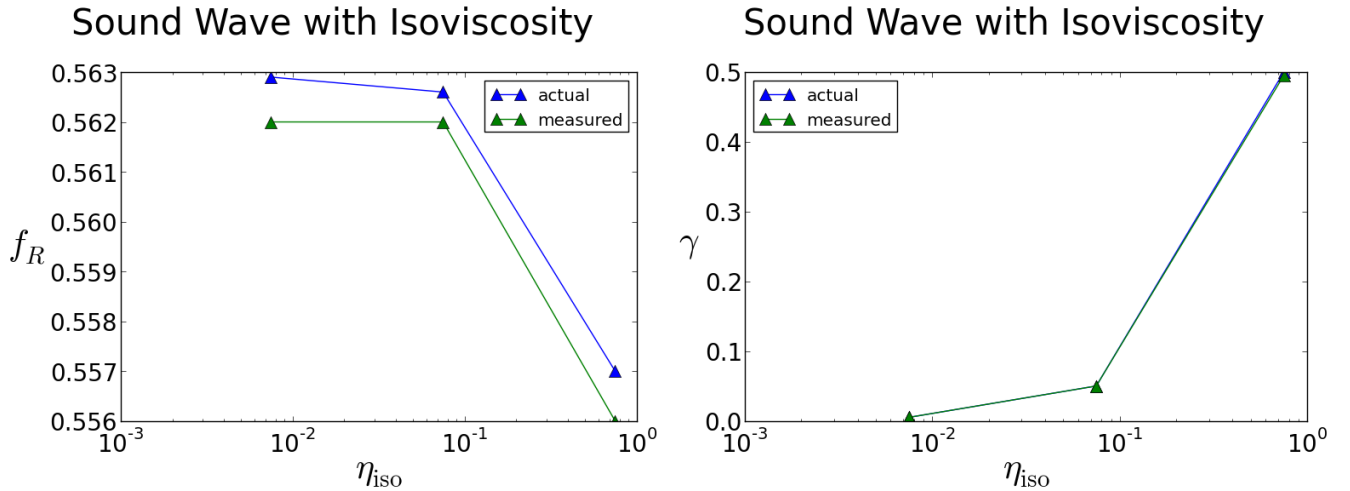


Figure 1: The frequency and damping rate for isoviscosity only for the sound wave.

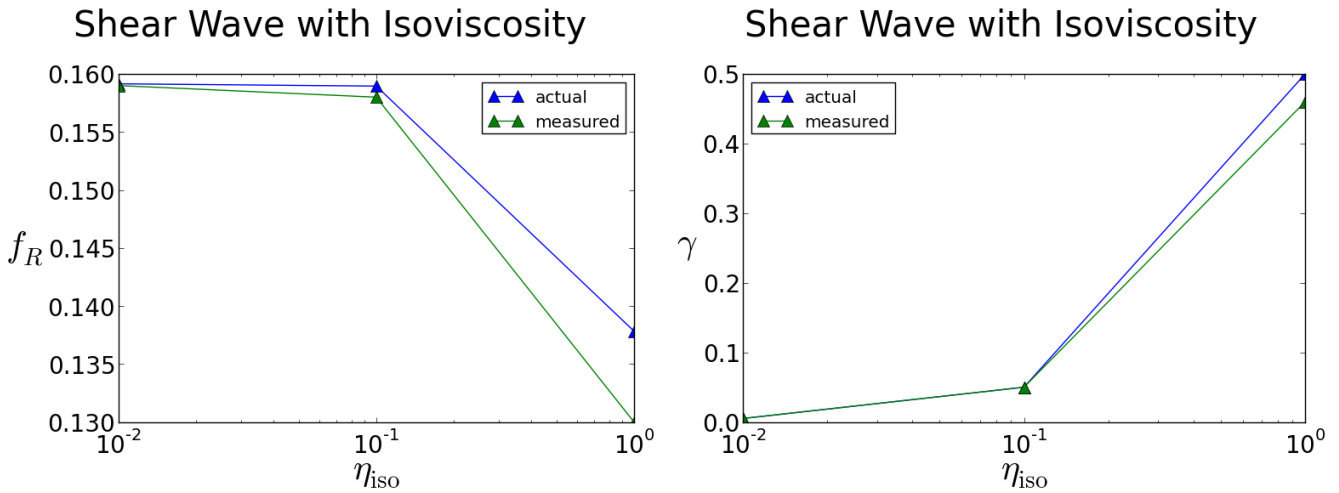


Figure 2: The frequency and damping rate for isoviscosity only for the shear wave.

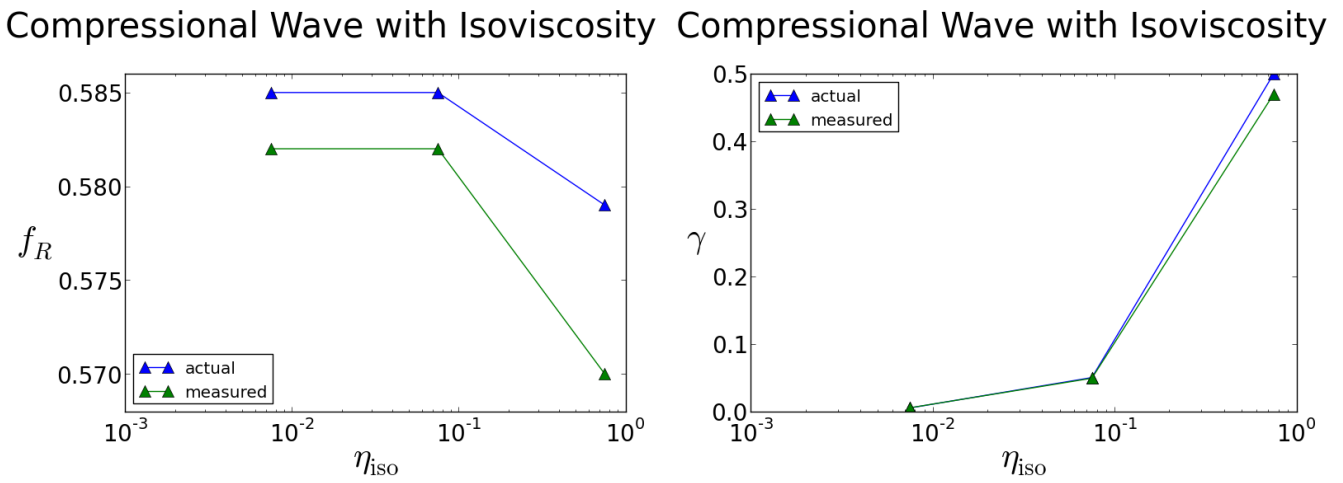


Figure 3: The frequency and damping rate for isoviscosity only for the compressional wave.

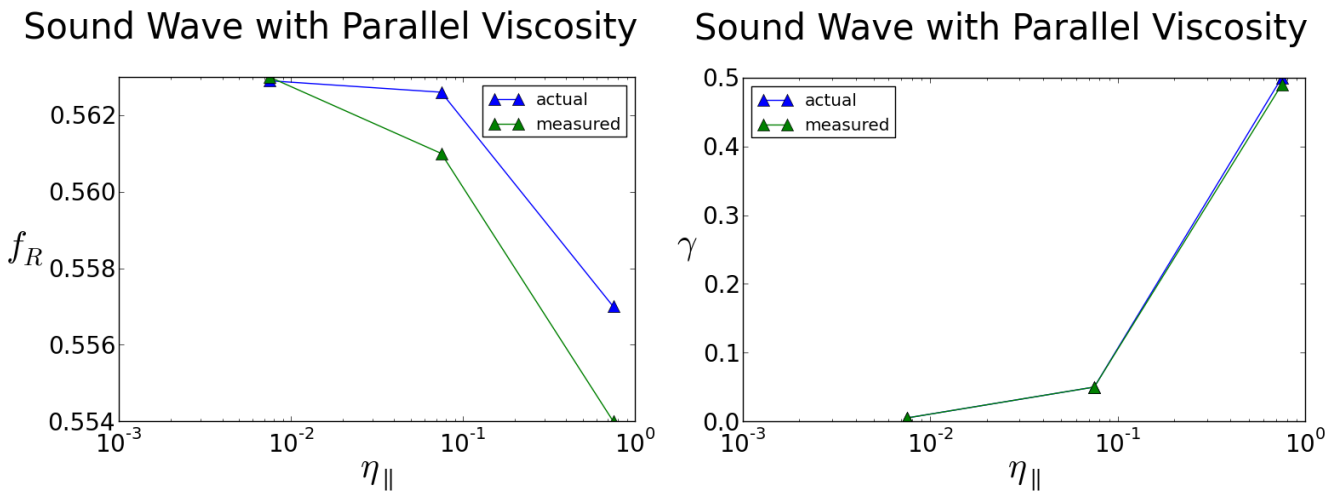
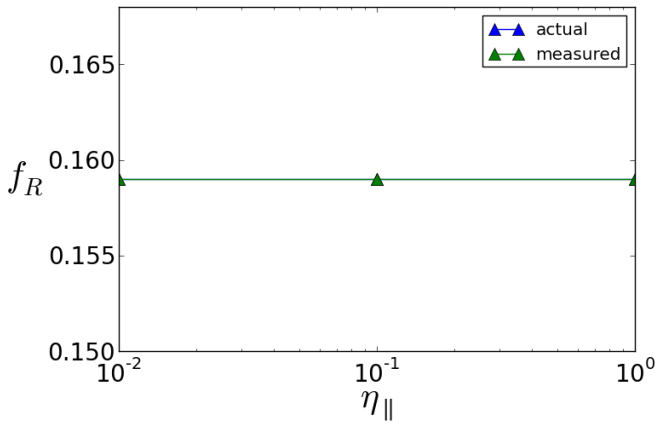


Figure 4: The frequency and damping rate for parallel viscosity only for the sound wave.

Shear Wave with Parallel Viscosity



Shear Wave with Parallel Viscosity

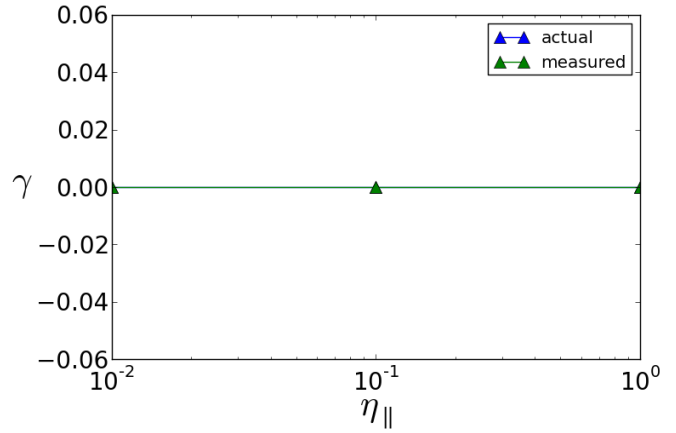
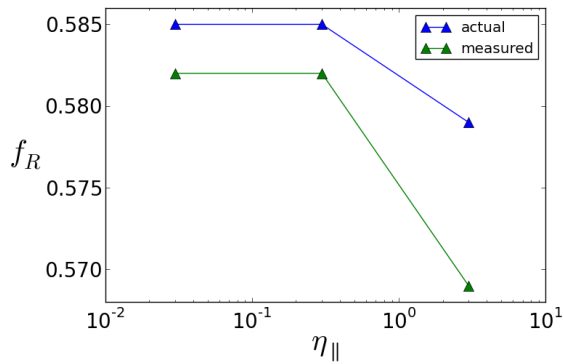


Figure 5: The frequency and damping rate for parallel viscosity only for the shear wave.

Compressional Wave with Parallel Viscosity



Compressional Wave with Parallel Viscosity

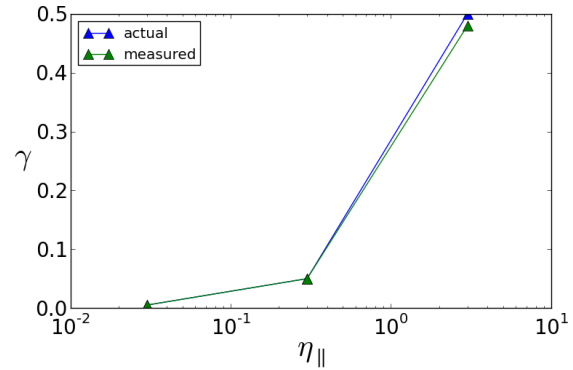
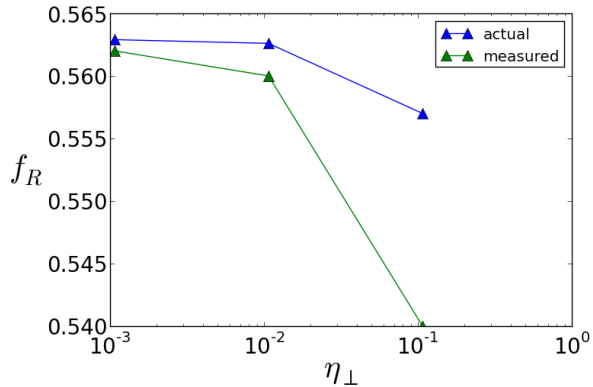


Figure 6: The frequency and damping rate for parallel viscosity only for the compressional wave.

Sound Wave with Perpendicular Viscosity



Sound Wave with Perpendicular Viscosity

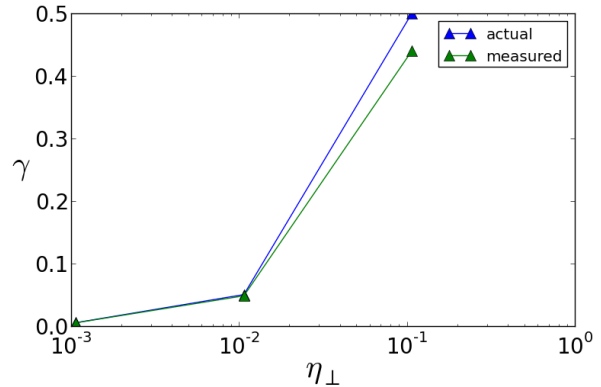


Figure 7: The frequency and damping rate for perpendicular viscosity only for the sound wave.

Shear Wave with Perpendicular Viscosity Shear Wave with Perpendicular Viscosity

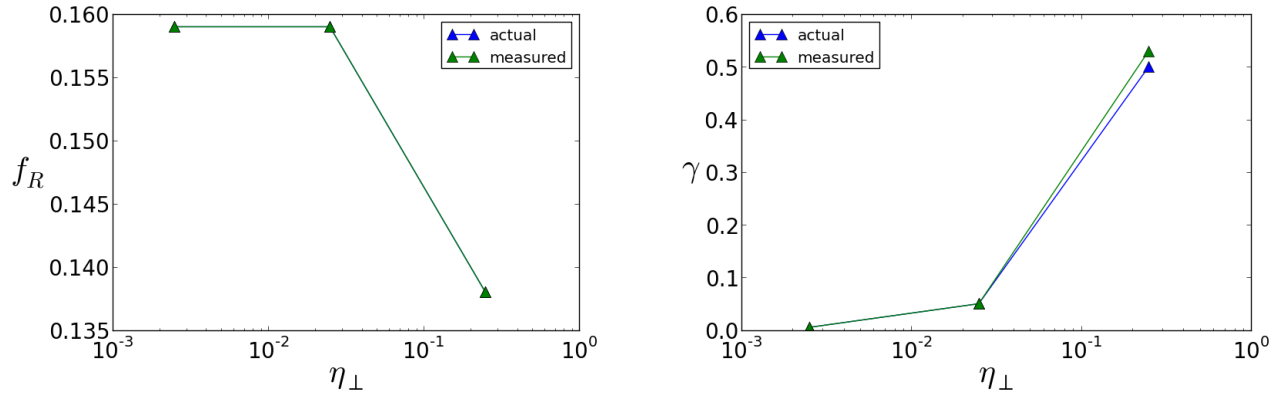


Figure 8: The frequency and damping rate for perpendicular viscosity only for the shear wave.

Compressional Wave with Perpendicular Viscosity Compressional Wave with Perpendicular Viscosity

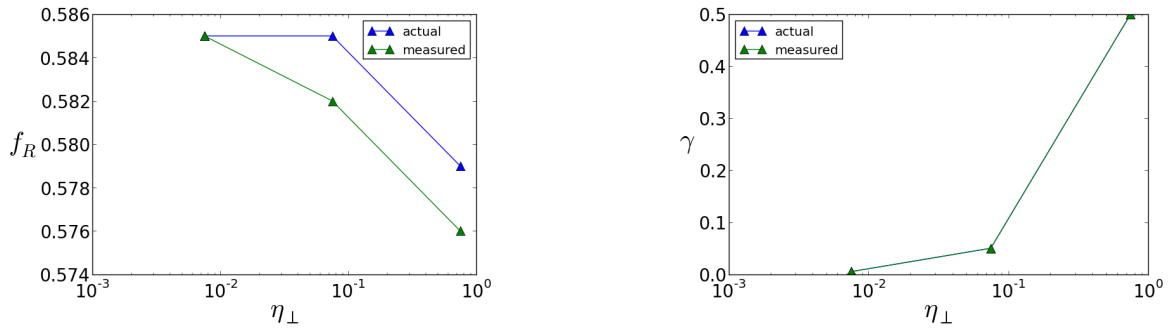
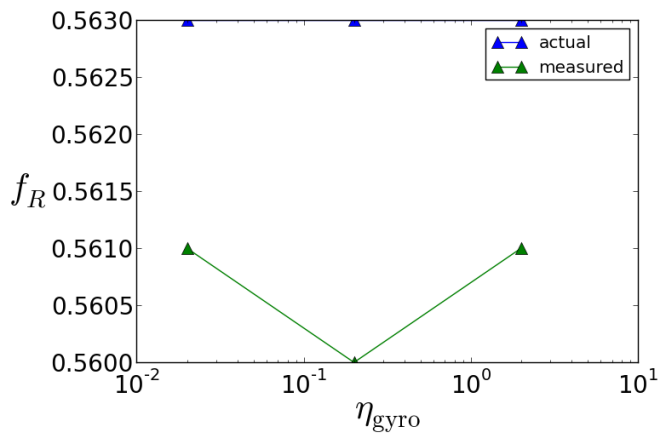


Figure 9: The frequency and damping rate for perpendicular viscosity only for the compressional wave.

Sound Wave with Gyroviscosity



Sound Wave with Gyroviscosity

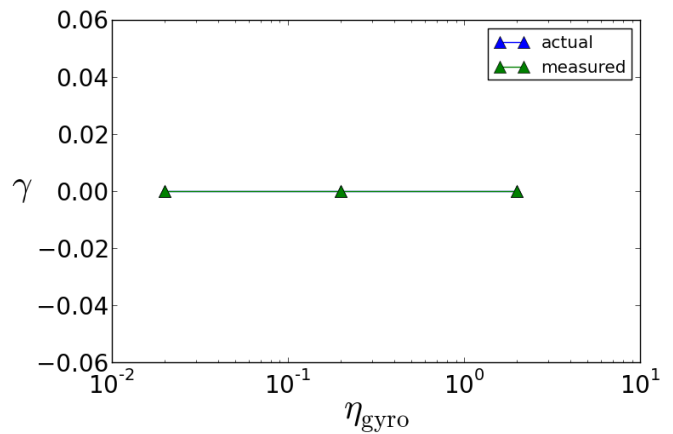


Figure 10: The frequency and damping rate for gyroviscosity only for the sound wave.

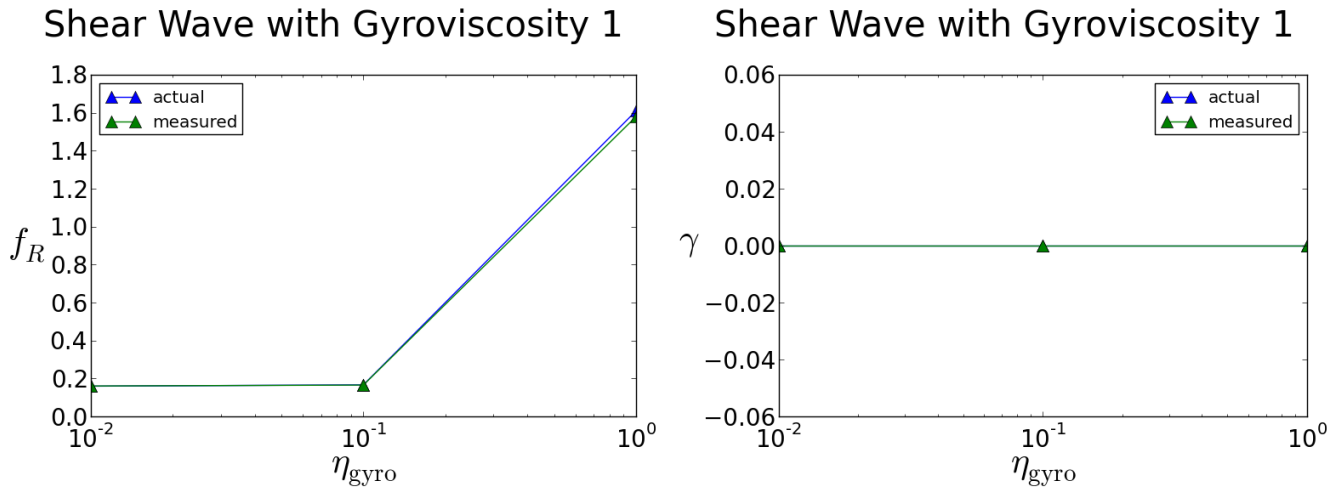


Figure 11: The frequency and damping rate for gyroviscosity only for the shear wave. (This is taking the higher frequency analytic value.)

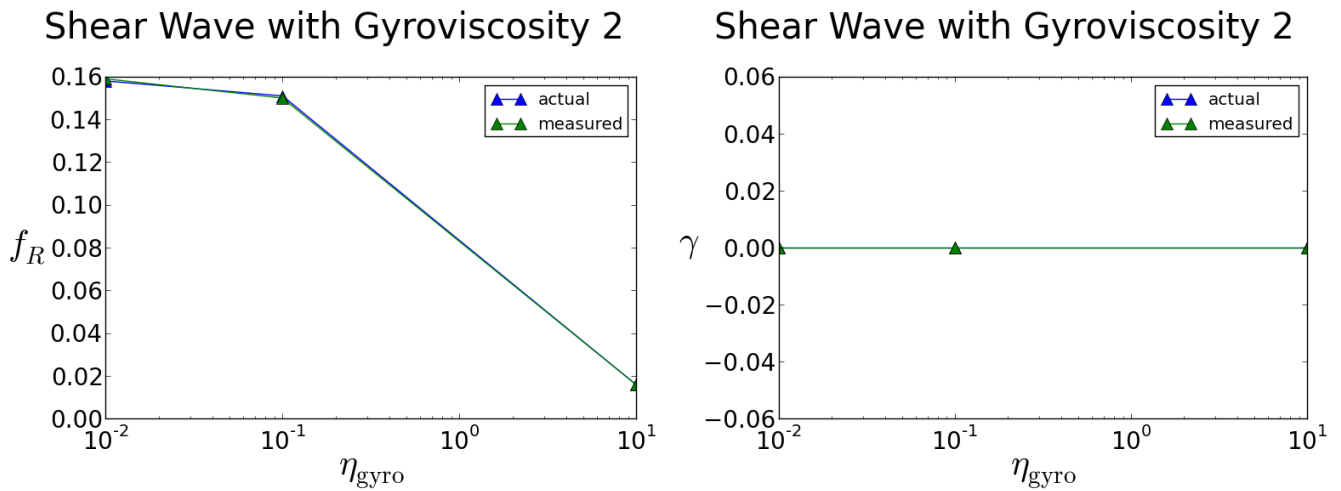


Figure 12: The frequency and damping rate for gyroviscosity only for the shear wave. (This is taking the higher frequency analytic value.)

Compressional Wave with Gyroviscosity Compressional Wave with Gyroviscosity

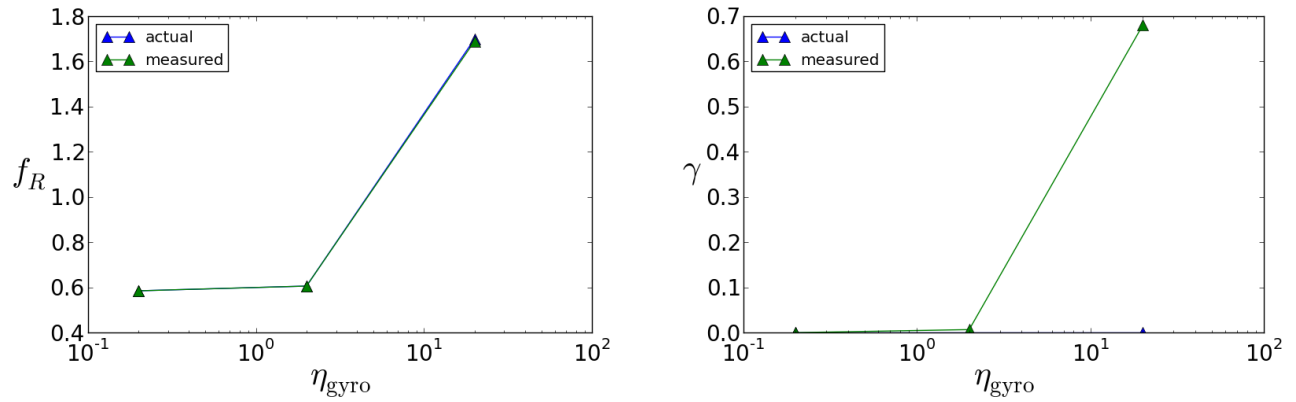


Figure 13: The frequency and damping rate for gyroviscosity only for the compressional wave. Note that the frequencies are quite accurate, but we get damping that is not apparent in the analytic relation.

3 NIMROD Calculations Run Nonlinearly

Let's now test the viscous Braginskii low and high magnetization limits with NIMROD run nonlinearly, which is available for nonlinear computations only. (Note that $\mathbf{k}_{\perp i} = k_{\perp, i} \lll 1$ and $\mathbf{k}_{\parallel e} = k_{\parallel, e} \ll 1$ must be chosen so that thermal diffusive effects are unimportant. In fact, $k_{\perp} = k_{\parallel} = 0$ is a possible choice. This is an artificial scaling, as for pure Braginskii, our implementation should keep these coefficients equal to unity.)

We have

$$\overleftrightarrow{\mathbf{\Pi}} = -\eta_0 \overleftrightarrow{\mathbf{W}}_{\parallel} - \eta_1 \overleftrightarrow{\mathbf{W}}_{\perp} + \eta_3 \overleftrightarrow{\mathbf{W}}_{\text{gyro}} \quad (68)$$

with

$$\overleftrightarrow{\mathbf{W}} = \nabla \mathbf{V} + (\nabla \mathbf{V})^{\top} - \frac{2}{3} \nabla \cdot \mathbf{V} \quad (69)$$

$$\overleftrightarrow{\mathbf{W}}_{\parallel} = \frac{3}{2} (\overleftrightarrow{\mathbf{W}} : \hat{\mathbf{b}} \hat{\mathbf{b}}) (\hat{\mathbf{b}} \hat{\mathbf{b}} - \mathbb{1}/3) \quad (70)$$

$$\overleftrightarrow{\mathbf{W}}_{\perp} = (\mathbb{1} + \kappa_{\perp} \hat{\mathbf{b}} \hat{\mathbf{b}}) \cdot \overleftrightarrow{\mathbf{W}} \cdot (\mathbb{1} + \kappa_{\perp} \hat{\mathbf{b}} \hat{\mathbf{b}}) + \frac{1}{2} (\mathbb{1} + \kappa_{\vee} \hat{\mathbf{b}} \hat{\mathbf{b}}) (\hat{\mathbf{b}} \hat{\mathbf{b}} : \overleftrightarrow{\mathbf{W}}) \quad (71)$$

$$\overleftrightarrow{\mathbf{W}}_{\text{gyro}} = \frac{1}{2} \left[(\hat{\mathbf{b}} \times \overleftrightarrow{\mathbf{W}}) \cdot (\kappa_{\wedge} \hat{\mathbf{b}} \hat{\mathbf{b}} + \mathbb{1}) - (\kappa_{\wedge} \hat{\mathbf{b}} \hat{\mathbf{b}} + \mathbb{1}) \cdot (\overleftrightarrow{\mathbf{W}} \times \hat{\mathbf{b}}) \right] \quad (72)$$

where, using Braginskii notation,

$$\kappa_{\perp} = \frac{\eta_2}{\eta_1} - 1 \equiv \gamma_{\perp} - 1 \quad (73)$$

$$\kappa_{\vee} = -2 \left(\frac{\eta_2}{\eta_1} \right)^2 - 1 \equiv -2\gamma_{\perp}^2 - 1 \quad (74)$$

$$\kappa_{\wedge} = 2 \frac{\eta_4}{\eta_3} - 1 \equiv 2\gamma_{\wedge} - 1 \quad (75)$$

We can note again that the implementation of $\overleftrightarrow{\mathbf{W}}_{\perp, \parallel}$ is actually that used above for $\overleftrightarrow{\mathbf{\Pi}}_{\perp, \parallel}^b$, although this will make no difference for these calculations as we do not isolate each tensor component's effects, so that when we add all components of the tensor together to form the full stress tensor we get the same result.

This also leads to the dispersion relation for sound waves ($\mathbf{k} = k_{\parallel} \hat{\mathbf{b}}$, $\mathbf{V} = v_{\parallel} \hat{\mathbf{b}}$) becoming

$$\omega^2 + i\omega k_{\parallel}^2 \left(\hat{\eta}_{\text{kin}} + \frac{4}{3} \hat{\eta}_{\text{iso}} + \frac{4}{3} \hat{\eta}_{\parallel} \right) - k_{\parallel}^2 v_S^2 = 0 \quad (76)$$

because we are not isolating out \perp , \parallel and gyro components individually.

Similarly, the dispersion relation for compressional Alfvén waves becomes ($\mathbf{k} \cdot \hat{\mathbf{b}} = 0$, $\mathbf{V} \cdot \hat{\mathbf{b}} = 0$, letting $\hat{\mathbf{b}} = \hat{\mathbf{z}}$)

$$\begin{aligned} \omega^4 + i\omega^3 F^2 - \omega^2 (v_W^2 k^2 + F_x F_y + \hat{\eta}_{\text{gyro}}^2 k^4 - \delta^2 k_x^2 k_y^2) \\ - i\omega v_W^2 (F_x k_y^2 + F_y k_x^2 - 2\delta k_x^2 k_y^2) = 0 \end{aligned} \quad (77)$$

where

$$F_i = k^2(\widehat{\eta}_{\text{kin}} + \widehat{\eta}_{\text{iso}} + \widehat{\eta}_{\perp}) + \frac{\widehat{\eta}_{\text{iso}} + \widehat{\eta}_{\parallel}}{3} k_i^2 \quad (78)$$

$$F^2 = 2k^2(\widehat{\eta}_{\text{kin}} + \widehat{\eta}_{\text{iso}} + \widehat{\eta}_{\perp}) + k^2 \frac{\widehat{\eta}_{\text{iso}} + \widehat{\eta}_{\parallel}}{3} \quad (79)$$

$$\delta = \frac{\widehat{\eta}_{\text{iso}} + \widehat{\eta}_{\parallel}}{3} \quad (80)$$

$$v_W^2 = v_A^2 + v_S^2 \quad (81)$$

In the high magnetization limit, $\eta_4 = 2\eta_3$ and $\eta_2 = 4\eta_1$. Let the (ion) magnetization be defined as $x_i \equiv \Omega_i \tau_i$, with NIMROD implementations as

$$\Omega_i = \frac{q_i B_0}{m_i} \quad (82)$$

$$\tau_i = \frac{12\pi^{3/2} m_i^{1/2} (k_B T_i / T_{\text{ref}})^{3/2} \epsilon_0^2 Z_{\text{eff}}}{n_i q_i^4 \ln \Lambda} \quad (83)$$

If we decide to use $\ln \Lambda$ as implemented in NIMROD, we have

$$\frac{1}{\lambda_D^2} = \frac{n}{\epsilon_0 k_B} \left(\frac{q_i^2}{Z_{\text{eff}} T_i} + \frac{q_e^2}{T_e} \right) \quad (84)$$

$$\ln \Lambda_{ii} = \ln \left(\frac{24\pi\epsilon_0}{q_i^2} k_B T_i \lambda_D \right) \quad (85)$$

For this scan, we will just set $\ln \Lambda_{ii} = 1$, as it will make little difference. Thus, we keep the default of `coulomb_logarithm = 1`. NIMROD also has `magfac_ele = g_e` and `magfac_ion = g_ion` which we can use to change our magnetization limit rather than directly changing it through T_i and B_0 as we would normally have to do.

Let's use the normalizations

$$m_i = c = \mu_0 = k_B = q = 1 \quad (86)$$

$$m_e = 10^{-3} \quad (87)$$

or (also note that $\epsilon_0 = 1/\sqrt{c^2\mu_0}$)

$$\text{mi_input} = \text{kblz_input} = \text{mu0_input} = \text{chrg_input} = \text{c_input} = 1 \quad (88)$$

$$\text{me_input} = 10^{-3} \quad (89)$$

Let's choose

$$\beta = \text{beta} = 15 \quad (90)$$

$$B_0 = \text{be0} = 1 \quad (91)$$

$$n_0 = \text{ndens} = 1 \quad (92)$$

Leaving the default adiabatic index of $\gamma = 5/3$, this then leads to (with `pe_frac = 0.5`)

$$v_A^2 = \frac{B_0^2}{(m_i + m_e)\mu_0 n_0} = \frac{1^2}{(1 + 10^{-3})(1)(1)} = \frac{1000}{1001} = 0.\overline{999000} \quad (93)$$

$$p_0 = \frac{\beta}{2\mu_0} = \frac{15}{2(1)} = 7.5 \quad (94)$$

$$T_0 = \frac{p_0}{n_0} = \frac{7.5}{1} = 7.5 \quad (95)$$

$$T_i = (1 - \text{pe_frac})T_0 = \frac{15}{4} = 3.75 = T_e \quad (96)$$

$$v_S^2 = \frac{\gamma T_0}{m_i} = B_0^2 \frac{\gamma \beta}{2\mu_0 n_0 (m_i + m_e)} = 1^2 \frac{\frac{5}{3}15}{4(1)(1)(1 + 10^{-3})} = \frac{12500}{1001} = 12.4875 \quad (97)$$

Note we can use a parallel reference temperature. Setting `k_parallel_ref_t` $\equiv T_{\text{ref}} = 0.375 = T_i$ simplifies the temperature dependence (this sets $T_i = 1$ in our calculations).

Let us remind ourselves of the effect of thermal diffusivity parameters. In order to isolate viscous effects, we choose $k_{\perp} = \text{k_perpi} = 10^{-8}$ and $k_{\parallel} = \text{k_plle} = 10^{-4}$ so that thermal effects are negligible (this is an artificial scaling), and the dispersion relations remain in the viscous MHD regime considered above. Note that $k_{\perp} = k_{\parallel} = 0$ is also allowed.

With this choice of parameters, we have $\Omega_i = 1$, and

$$\frac{\tau_i}{(k_B T_i / T_{\text{ref}})^{3/2}} = \frac{12\pi^{3/2}}{1} \approx 66.8199 \quad (98)$$

Thus, we begin at $x_i = 66.8199(T_i / T_{\text{ref}})$ as our default magnetization.

Take $T_{\text{ref}} = 37.5$ so that $T_i / T_{\text{ref}} = 0.1$ and we get

$$x_i = 66.8199(0.1)^{3/2} \approx 2.113031907464526 \quad (99)$$

We then have

$$\eta_0 = \text{par_visc} \frac{T_i}{T_{\text{ref}}} \frac{\tau_i}{m_i} \frac{\gamma_0}{\delta_0} \quad (100)$$

$$\eta_1(x_i) = \text{prp_visc} \eta_2(2x_i) \quad (101)$$

$$\eta_2(x_i) = \text{prp_visc} \frac{T_i}{T_{\text{ref}}} \frac{\tau_i}{m_i} \frac{\gamma_1 x_i^2 + \gamma_0}{x_i^4 + \delta_1 x_i^2 + \delta_0} \quad (102)$$

$$\eta_3(x_i) = \text{gyr_visc} \eta_4(2x_i) \quad (103)$$

$$\eta_4(x_i) = \text{gyr_visc} \frac{T_i}{T_{\text{ref}}} \frac{\tau_i}{m_i} x_i \frac{\sigma_1 x_i^2 + \sigma_0}{x_i^4 + \delta_1 x_i^2 + \delta_0} \quad (104)$$

This then requires `par_visc = prp_visc = gyr_vis = 1` unless artificially scaling coefficients. See the `nimrod.in` for the numerical values of the parameters above (namely, $\gamma_0, \delta_0, \gamma_1, \delta_1, \sigma_1, \sigma_0$). Note again we can scale x_i through `magfac_ion` $\equiv g_{\text{ion}}$.

For the following figures we scale x_i through g_{ion} from the low-magnetization to high-magnetization limit. ‘‘Actual’’ comes from the analytic dispersion relation, while ‘‘measured’’ is from NIMROD output.

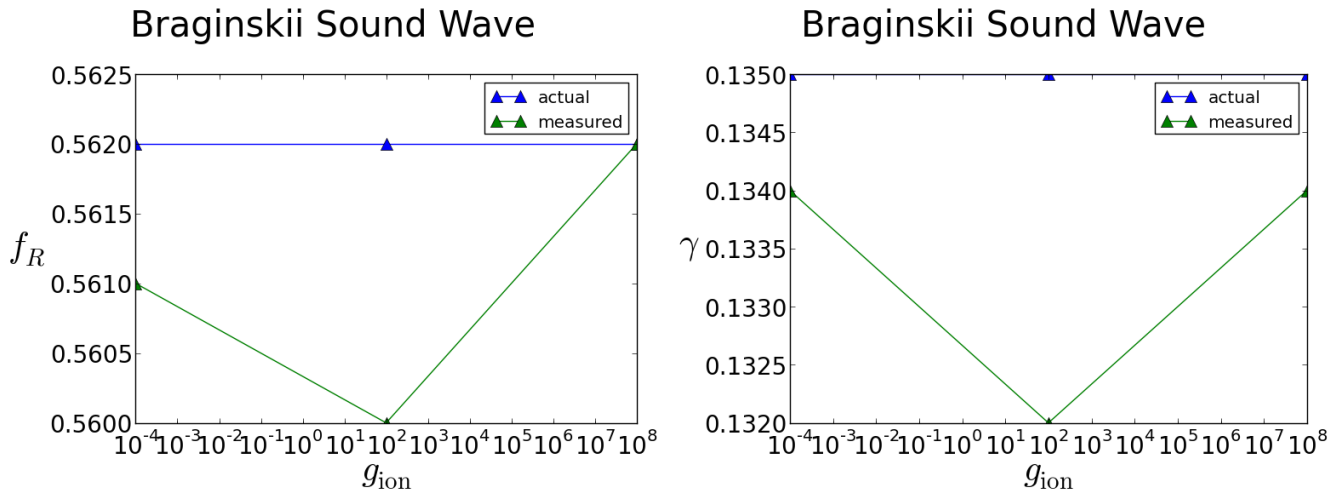


Figure 14: The frequency and damping rate for Braginskii parameters quoted above for various g_{ion} for the sound wave.

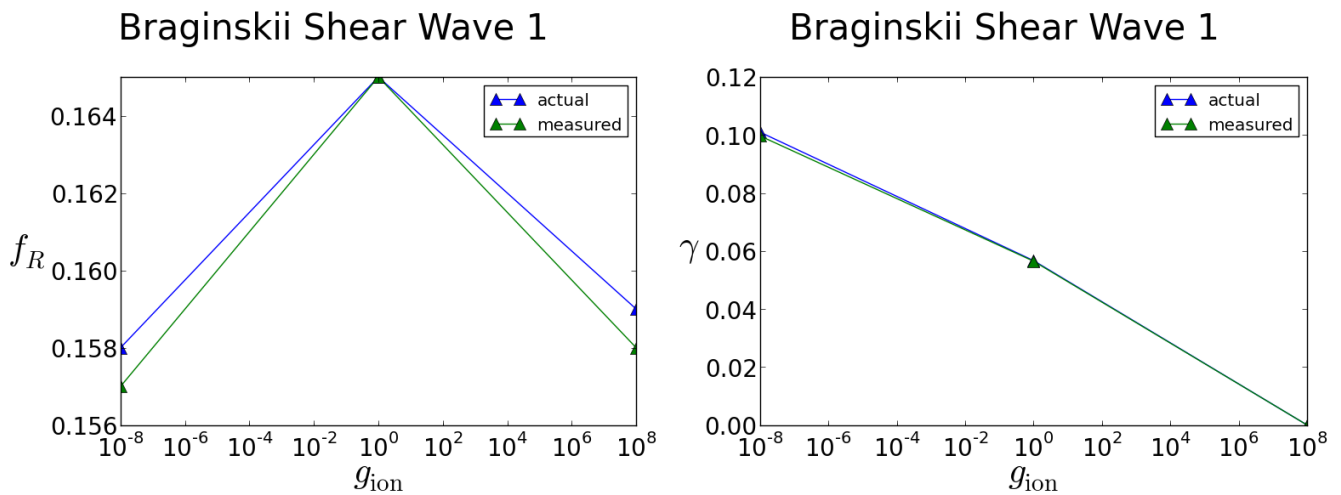


Figure 15: The frequency and damping rate for Braginskii parameters quoted above for various g_{ion} for the shear wave (the “upper” branch in frequency). Note the damping rate for the $g_{ion} = 1$ is not the actual damping rate, it is simply a measure of damping.

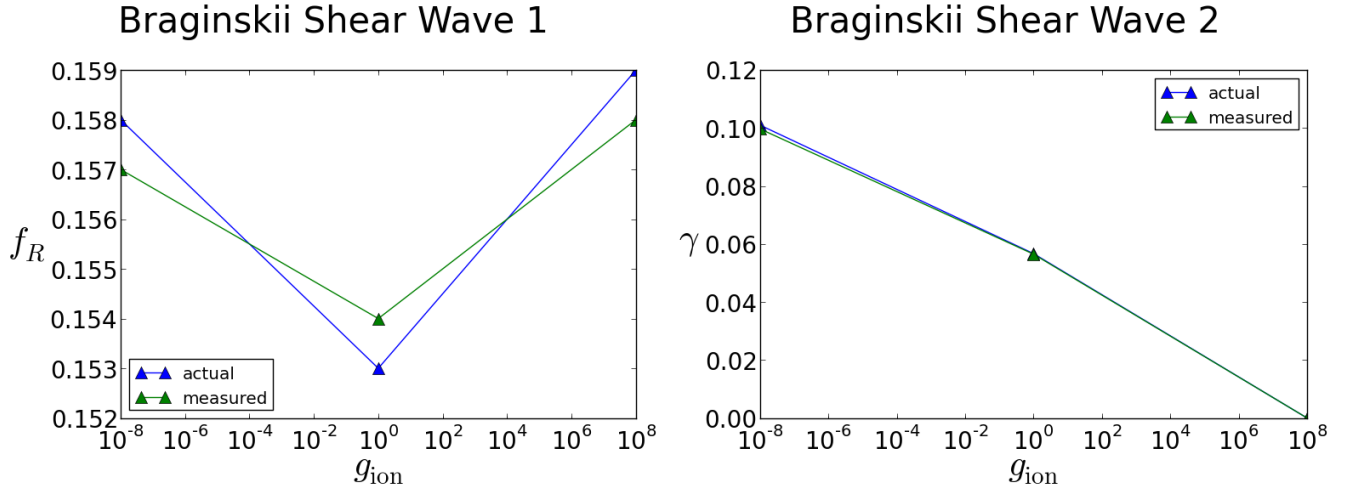


Figure 16: The frequency and damping rate for Braginskii parameters quoted above for various g_{ion} for the shear wave (the “lower” branch in frequency). Note the damping rate for the $g_{ion} = 1$ is not the actual damping rate, it is simply a measure of damping.

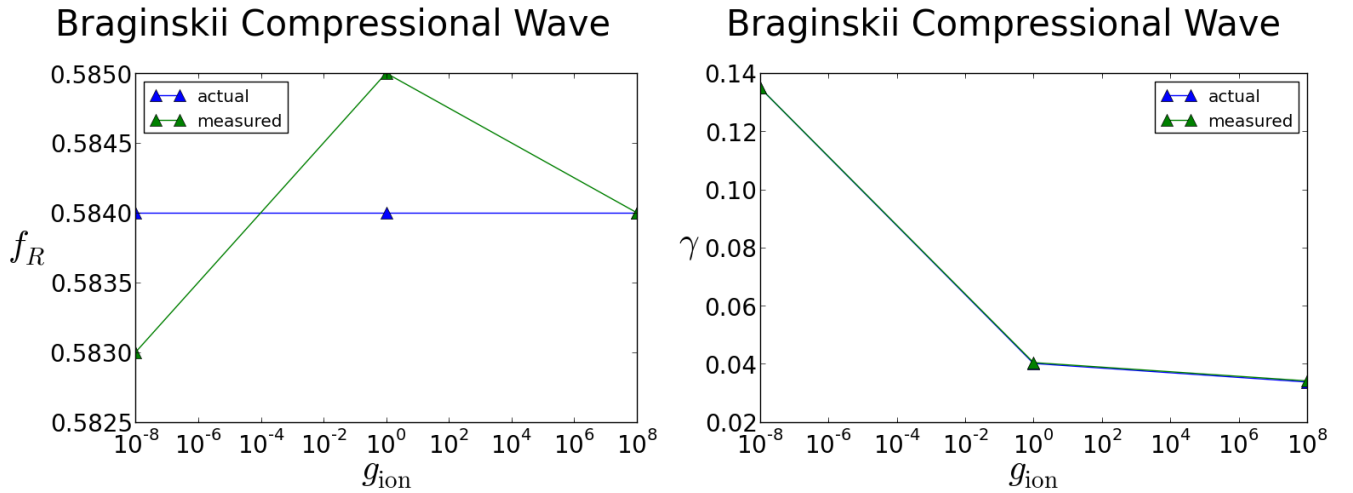


Figure 17: The frequency and damping rate for Braginskii parameters quoted above for various g_{ion} for the compressional wave.

4 Full Braginskii Closure Test

We modify our system (we will still test NIMROD evolving only a single temperature)

$$\frac{\partial n}{\partial t} + \nabla \cdot (n\mathbf{V}) = 0 \quad (105)$$

$$mn \frac{\partial \mathbf{V}}{\partial t} + mn \mathbf{V} \cdot \nabla \mathbf{V} = \mathbf{J} \times \mathbf{B} - \nabla \cdot \overset{\leftrightarrow}{\mathbf{P}} \quad (106)$$

$$n_s \frac{dT_s}{dt} = -(\gamma - 1)n_s T_s \nabla \cdot \mathbf{V} - (\gamma - 1) \nabla \cdot \mathbf{q}_s + (\gamma - 1) Q_s \quad (107)$$

$$\mu_0 \mathbf{J} = \nabla \times \mathbf{B} \quad (108)$$

$$\mathbf{E} = -\mathbf{V} \times \mathbf{B} \quad (109)$$

$$\frac{\partial \mathbf{B}}{\partial t} = -\nabla \times \mathbf{E} \quad (110)$$

$$\nabla \cdot \mathbf{B} = 0 \quad (111)$$

where γ is the adiabatic index, set to 5/3 in usual MHD circumstances and s is a species index. Our closure in this case becomes

$$\overleftrightarrow{\mathbf{P}} = \mathbb{1}p + \sum_s \overleftrightarrow{\mathbf{\Pi}}_s \quad (112)$$

$$p = \sum_s n_s T_s \quad (113)$$

$$-\nabla \cdot \mathbf{q}_s = \chi_{\parallel,s} \nabla_{\parallel} T_s + \chi_{\perp,s} \nabla_{\perp} T_s + \chi_{\wedge,s} \hat{\mathbf{b}} \times \nabla T_s \quad (114)$$

Note that $\overleftrightarrow{\mathbf{\Pi}}_e$ is conventionally ignored, as $\overleftrightarrow{\mathbf{\Pi}}_i \gg \overleftrightarrow{\mathbf{\Pi}}_e$. In NIMROD we only calculate ion contributions to $\overleftrightarrow{\mathbf{\Pi}}$. From now on, let's drop the species indices for the rest of this calculation.

The only difference in the linearization, is that we find

$$\frac{T_0}{T_1} = \frac{(\gamma - 1)(\mathbf{k} \cdot \mathbf{V}_1)}{\omega + i(\bar{\chi}_{\parallel} k_{\parallel}^2 + \bar{\chi}_{\perp} k_{\perp}^2)} \quad (115)$$

where $\bar{\chi} = (\gamma - 1)\chi/n_0$.

This leads to the same dispersion relations as before, except

$$v_S^2 \rightarrow \frac{v_S^2}{\gamma} \left[1 + \frac{(\gamma - 1)}{1 + ik_l^2 \bar{\chi}_l / \omega} \right] \quad (116)$$

where the l is either \perp or \parallel depending on \mathbf{k} for the dispersion relation. Thus define

$$\bar{v}_S^2 = \frac{v_S^2}{\gamma} \left[1 + \frac{(\gamma - 1)}{1 + ik_l^2 \bar{\chi}_l / \omega} \right] \quad (117)$$

$$\bar{v}_W^2 = v_A^2 + \bar{v}_S^2 \quad (118)$$

Thus, the dispersion relation for sound waves ($\mathbf{k} = k_{\parallel} \hat{\mathbf{b}}$, $\mathbf{V} = v_{\parallel} \hat{\mathbf{b}}$) is

$$\omega^2 + i\omega k_{\parallel}^2 \left(\hat{\eta}_{\text{kin}} + \frac{4}{3} \hat{\eta}_{\text{iso}} + \frac{4}{3} \hat{\eta}_{\parallel} \right) - k_{\parallel}^2 \bar{v}_S^2 = 0 \quad (119)$$

The dispersion relation for shear Alfvén waves ($\mathbf{k} = k_{\parallel} \hat{\mathbf{b}}$, $\mathbf{V} \cdot \hat{\mathbf{b}} = 0$) yields (it is unaffected by thermal diffusion)

$$(\omega^2 - k_{\parallel}^2 v_A^2 + i\omega k_{\parallel}^2 \hat{\eta}_{\text{eff}} - \alpha_{\wedge} \omega k_{\parallel}^2 \hat{\eta}_{\text{gyro}})(\omega^2 - k_{\parallel}^2 v_A^2 + i\omega k_{\parallel}^2 \hat{\eta}_{\text{eff}} + \alpha_{\wedge} \omega k_{\parallel}^2 \hat{\eta}_{\text{gyro}}) = 0 \quad (120)$$

$$\hat{\eta}_{\text{eff}} = \hat{\eta}_{\text{kin}} + \hat{\eta}_{\text{iso}} + \hat{\eta}_{\perp} (1 + \kappa_{\perp}) \quad (121)$$

Similarly, the dispersion relation for compressional Alfvén waves becomes ($\mathbf{k} \cdot \hat{\mathbf{b}} = 0, \mathbf{V} \cdot \hat{\mathbf{b}} = 0$, letting $\hat{\mathbf{b}} = \hat{\mathbf{z}}$)

$$\omega^4 + i\omega^3 F^2 - \omega^2(v_W^2 k^2 + F_x F_y + \hat{\eta}_{\text{gyro}}^2 k^4 - \delta^2 k_x^2 k_y^2) - i\omega v_W^2 (F_x k_y^2 + F_y k_x^2 - 2\delta k_x^2 k_y^2) = 0 \quad (122)$$

where

$$F_i = k^2(\hat{\eta}_{\text{kin}} + \hat{\eta}_{\text{iso}} + \hat{\eta}_{\perp}) + \frac{\hat{\eta}_{\text{iso}} + \hat{\eta}_{\parallel}}{3} k_i^2 \quad (123)$$

$$F^2 = 2k^2(\hat{\eta}_{\text{kin}} + \hat{\eta}_{\text{iso}} + \hat{\eta}_{\perp}) + k^2 \frac{\hat{\eta}_{\text{iso}} + \hat{\eta}_{\parallel}}{3} \quad (124)$$

$$\delta = \frac{\hat{\eta}_{\text{iso}} + \hat{\eta}_{\parallel}}{3} \quad (125)$$

$$v_W^2 = v_A^2 + \bar{v}_S^2 \quad (126)$$

The χ coefficients now have dependencies on other parameters and are given by

$$\chi_{\parallel,s} = \frac{T_s \tau_s}{m_s} \frac{\gamma_{0,s}}{\delta_{0,s}} \quad (127)$$

$$\chi_{\perp,s} = \frac{T_s \tau_s}{m_s} \frac{\gamma_{1,s} x_s^2 + \gamma_{0,s}}{x_s^4 + \delta_{1,s} x_s^2 + \delta_{0,s}} \quad (128)$$

$$\tau_i = \sqrt{2} \tau_{ii} \quad (129)$$

$$\tau_e = \tau_{ei} \quad (130)$$

the same as given in Braginskii. Note that in the NIMROD implementation, one actually puts in a coefficient for $(\gamma - 1)\chi$ rather than χ itself (although for our full Braginskii model, this is not relevant). Look in the NIMROD `input.f` file for γ and δ coefficients.

Note that all input quantities are the same as the nonlinearly run NIMROD cases, except that we now leave $k_{\perp,s} = k_{\parallel,s} = 1$.

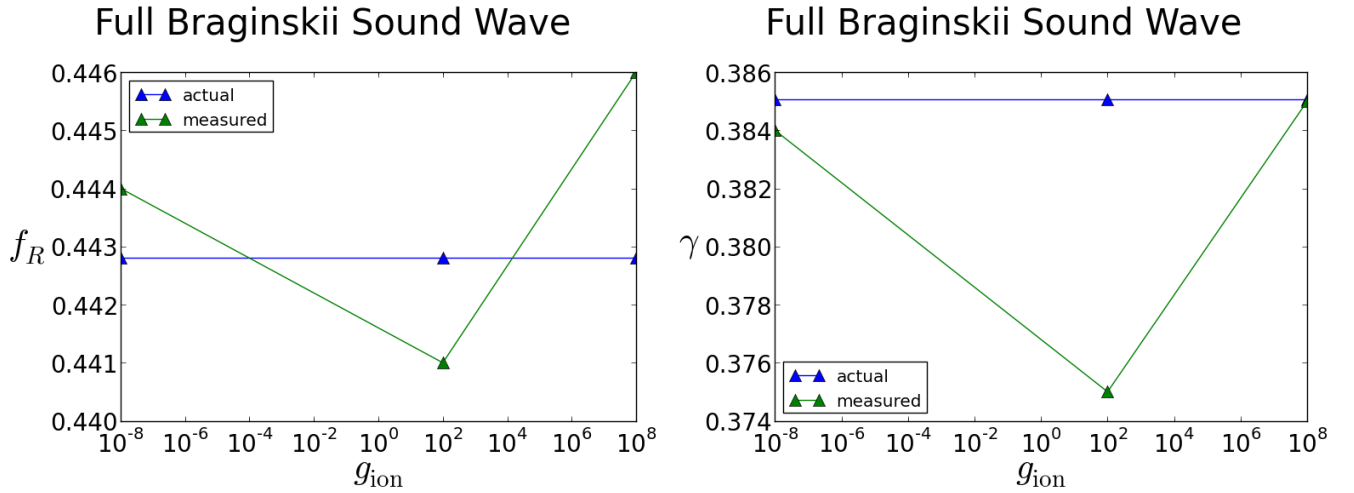


Figure 18: The frequency and damping rate for full Braginskii parameters quoted above for various g_{ion} for the sound wave.

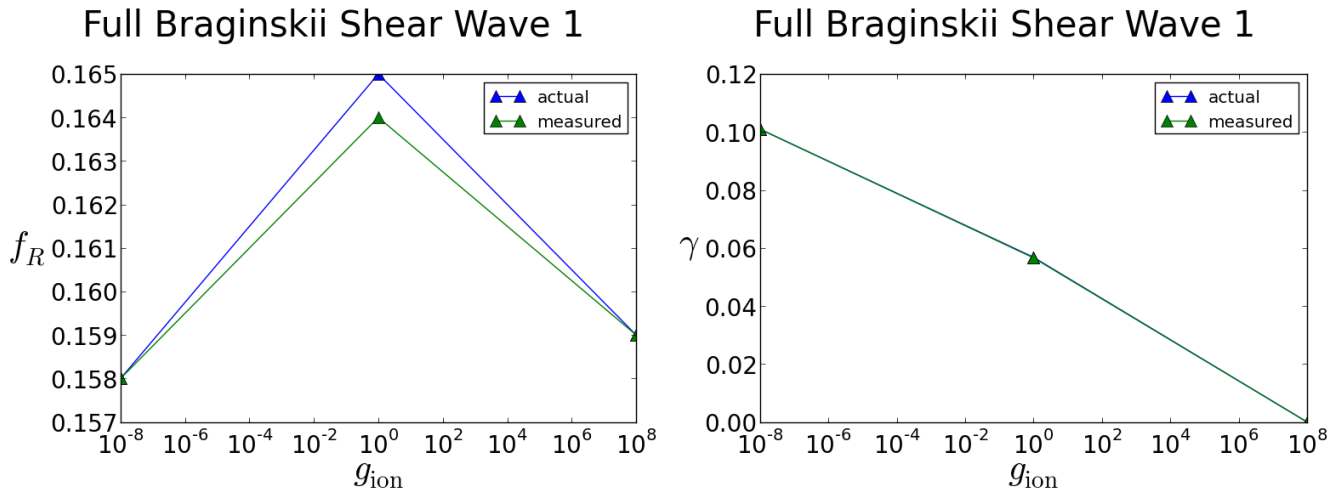


Figure 19: The frequency and damping rate for full Braginskii parameters quoted above for various g_{ion} for the shear wave (the “upper” branch in frequency). Note the damping rate for the $g_{ion} = 1$ is not the actual damping rate, it is simply a measure of damping.

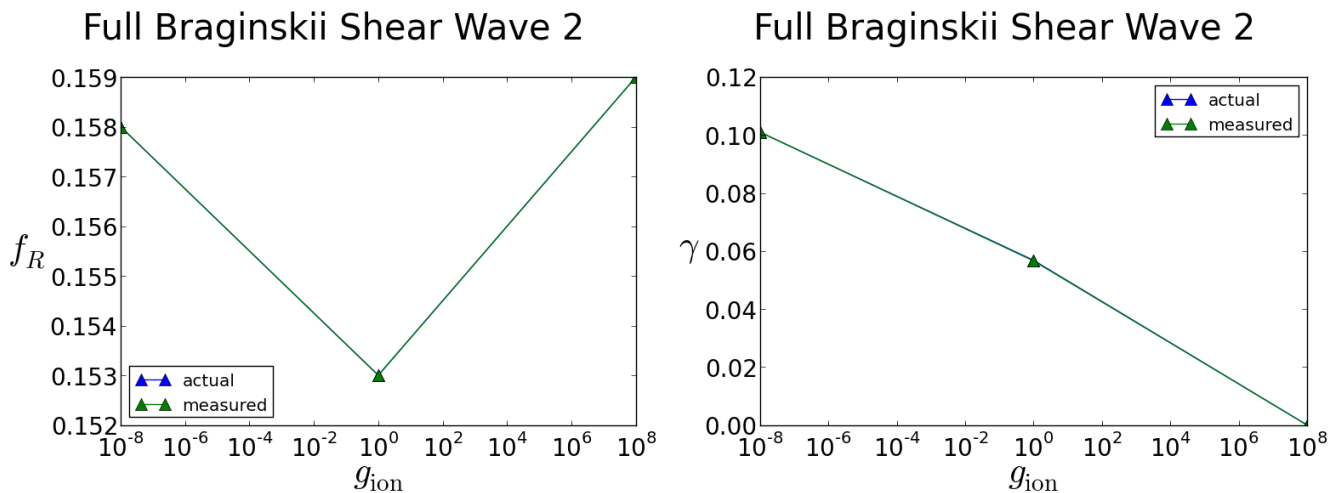


Figure 20: The frequency and damping rate for full Braginskii parameters quoted above for various g_{ion} for the shear wave (the “lower” branch in frequency). Note the damping rate for the $g_{ion} = 1$ is not the actual damping rate, it is simply a measure of damping.

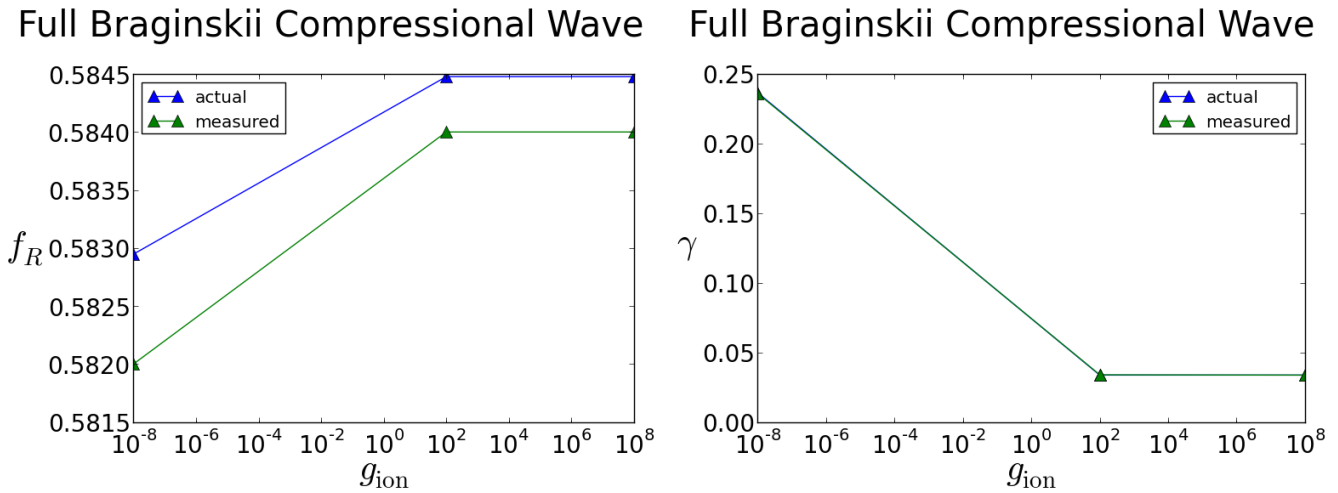


Figure 21: The frequency and damping rate for full Braginskii parameters quoted above for various g_{ion} for the compressional wave.

5 Temporal and Spatial Convergence Scan

We will use a linear isoviscous compressional wave as an example of the behavior found in general for temporal and spatial scans. In summary, the frequency converges rapidly as timestep is lowered, while increasing spatial resolution has little effect on convergence.

Compressional Wave with Isoviscosity Timestep Scan Compressional Wave with Isoviscosity Timestep Scan

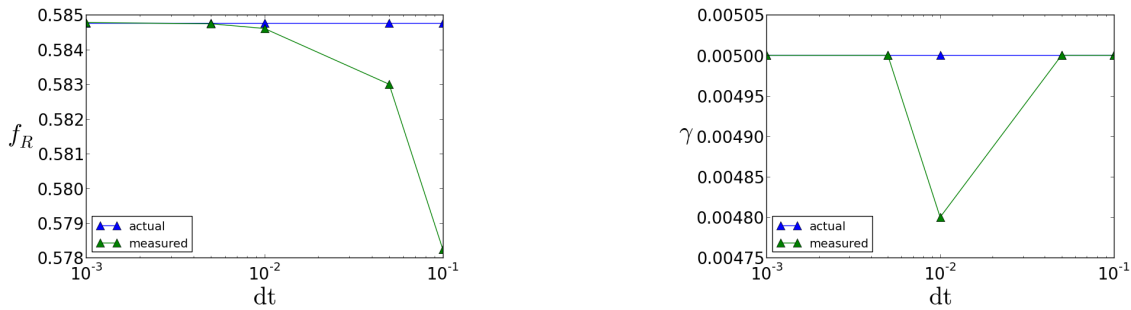


Figure 22: The frequency and damping rate for a linear isoviscously damped wave as a function of timestep size. Note that the error in the damping rate is mostly due to the difficulty of accurately measuring the small growth rate by eye.

Compressional Wave with Isoviscosity Spatial Scan

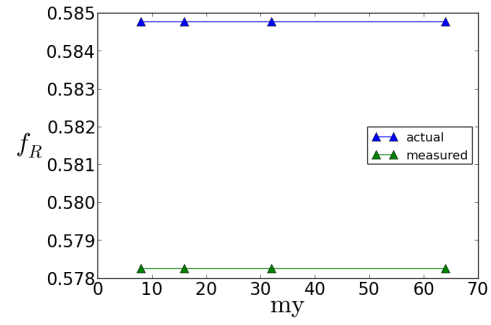


Figure 23: The frequency for a linear isoviscously damped wave as function of my (\hat{y} is the wave propagation direction).